# Chemically-induced Mobility Gaps in Graphene Nanoribbons: A Route for Upscaling Device Performances

Blanca Biel,[*,†,¶] François Triozon,[†] X. Blase,[‡] and Stephan Roche[§]

*CEA, LETI, MINATEC, F38054 Grenoble, France, Institut Néel, CNRS and Université Joseph Fourier, B.P. 166, 38042 Grenoble Cedex 09, France, and CEA, INAC/SPSMS/GT 17 rue des Martyrs, 38054 Grenoble Cedex 9, France*

E-mail:

**Abstract**

We report an *ab initio*-based study of mesoscopic quantum transport in chemically doped graphene nanoribbons with a width up to 10 nm. The occurrence of quasibound states related to boron impurities results in mobility gaps as large as 1 eV, driven by strong electron-hole asymmetrical backscattering phenomena. This phenomenon opens new ways to overcome current limitations of graphene-based devices through the fabrication of chemically-doped graphene nanoribbons with sizes within the reach of conventional lithography.

The basic principle of CMOS field effect transistor (CMOS-FET) is to drive a high current density in its ON-state, whereas electrostatic gating blocks almost completely the current flow in

[†]CEA, LETI, MINATEC, F38054 Grenoble, France

[‡]Institut Néel, CNRS and Université Joseph Fourier, B.P. 166, 38042 Grenoble Cedex 09, France

[§]CEA, INAC/SPSMS/GT 17 rue des Martyrs, 38054 Grenoble Cedex 9, France

[¶]Present address: Departamento de Electrónica y Tecnología de Computadores, Universidad de Granada, Campus de Fuente Nueva, and CITIC, Campus de Aynadamar, 18071 Spain

the so-called OFF-state. The current ratio between OFF and ON states is one of the key parameters determining the device performance.[1] This electrostatic control of the CMOS-FET is strongly efficient owing to the use of semiconducting materials, which present a sufficiently large electronic bandgap to electrostatically deplete or accumulate charges in the conducting channel. Recently, the synthesis of low dimensional carbon based materials has opened alternatives to silicon-based electronics devices. Indeed, by graphite exfoliation[2] or by sublimation of SiC,[3] the fabrication of single layer two-dimensional (2D) graphene or stacked graphene multilayers was achieved, with exceptionally high values of reported charge mobilities ($\geq 100.000$ cm$^2$V$^{-1}$s$^{-1}$) close to the Dirac point.[4,5,6] Notwithstanding, with 2D graphene being a zero-gap semiconductor,[7] a poor field effect efficiency with small ON/OFF current ratio was obtained.[4,5,6]

E-beam lithography and oxygen plasma etching allow to fabricate graphene nanoribbons (GNRs),[8,9,10] down to a few tens of nanometers in width, opening the possibility for bandgap engineering through electronic confinement. However, current limitations of state-of-the-art lithographic techniques hardly allow to fabricate GNRs with sufficiently large energy bandgaps.[11,12,13,14,15] To further reduce the GNRs lateral size down to a few nanometers, alternative chemical approaches have been developed and competitive device performances have been reported.[16,17] These approaches remain however hardly compatible with massive integration of interconnected devices at the wafer scale.

Chemical doping allows to develop new applications such as chemical sensors or more efficient electrochemical switches.[18,19] The conductivity modulation due to chemical doping and functionalization of 2D graphene has been explored numerically,[20,21] without showing significant improvement of device performances. Several theoretical studies have also investigated the effect of doping on the properties of single-layer GNRs. The impact of a single boron impurity on the electronic properties of GNRs was analyzed by first-principles methods in Refs.[22,23] Other works have considered the GNRs bandgap tuning by doping or functionalization,[24,25,26] but only gaps of a few tens of meV have been predicted. Theoretically, two types of GNRs with highly symmetric edges have been described, namely, zigzag (zGNRs) and armchair (aGNRs). To date, most efforts have focused on the spin-transport properties of zGNRs, while the possibilities for charge transport

of doped aGNRs have somehow been neglected. Besides, due to the computational cost of *ab initio* calculations, the width of the GNRs studied in those works is in general well below 3 nm.

In this Article, we report on a quantum transport study of chemically doped GNRs up to 10 nm in width. By combining first-principles calculations with tight-binding models, the effect of chemical doping on charge conduction is explored for ribbons with a length up to the micron and random distribution of substitutional boron impurities. The joint effects of backscattering together with the enhanced localization due to low dimensionality are shown to produce strong electron-hole transport asymmetry and large mobility gaps, even in the low doping limit. These chemically modified graphene-based materials, within reach of current lithographic techniques, should therefore allow for a strongly enhanced current density modulation under electrostatic gating.

We focus on the case of aGNRs. This type of ribbon symmetry has theoretically been proposed as energetically more stable and more resistant to edge defects when compared to zGNRs,[27,28,29] which seems to be confirmed by experimental observations.[30] As reported by *ab initio* calculations,[31,32,33] aGNRs are found to be always semiconducting with an energy gap that varies up to 0.5 eV for ribbons of similar width, depending on the exact number of dimer chains within the unit cell. Unlike zGNRs, the ground state of aGNRs is not spin-polarized. *p*-type (*n*-type) doping can be achieved by the incorporation of boron (nitrogen) atoms in substitution within the $sp^2$-type carbon matrix, as reported in Ref.[34] for carbon nanotubes and very recently in Ref.[35] in the case of 2D graphene. First-principles calculations of the effect of a single boron impurity on the electronic properties of aGNRs have been reported in Ref.[23] for aGNRs with widths between 2.3 and 4.2 nm. Following Ref.,[31] we refer to a aGNR with N dimers contained in its unit cell as an N-aGNR. Both types of possible electronic structures, namely the pseudo-metallic ribbons 20-aGNR and 35-aGNR (i.e., ribbons predicted to be metallic within a simple nearest-neighbor tight-binding model), and the semiconducting 34-aGNR were addressed. The modification of the electronic structure of the aGNRs by a single boron (or nitrogen) impurity turns out to be strongly dependent on the position of the dopant with respect to the ribbon edge, displaying a significant electron-hole asymmetry.[36,37] This phenomenon results from the interplay between wavefunction

symmetries and screening effects that are system-dependent. Regardless of their exact position across the ribbon width, boron impurities are found to preserve their well-known acceptor character (or hole-doping ability) in carbon, with vanishingly weak impact of the transport properties in the first conduction band close to the Fermi level ($E_F$), which almost preserves conductance quantization.

The large variation of resonant energies with the acceptor (donor) chemical impurity position allows however to infer that a random distribution of impurities will likely result in an uniform reduction of conductance over the occupied (unoccupied) states part of the first conduction *plateau*, yielding marked electron-hole asymmetry and charge mobility gaps intrinsic to p-type (n-type) doping. The present work is the first theoretical study based on *ab initio* atomistic models providing confirmation to such prediction.

Due to the large size of our unit cells, a statistical study of the mesoscopic transport using the fully *ab initio* Hamiltonian[38] is not possible here. We have used instead a combination of first-principles calculations with tight-binding models, that has been satisfactorily employed before for doped carbon nanotubes.[39] As a first step, the scattering potential induced by the dopant has been extracted from those first-principles density functional theory (DFT) calculations. The analysis of the *ab initio* onsite and hopping terms around the dopant, as obtained from self-consistent DFT calculations within an atomic-like basis, allows to build a simple nearest-neighbor tight-binding (nn-TB) model. The substitutional impurity modifies mainly the onsite terms, creating a potential well on a typical length scale of about 10 Angstrom (see Ref.[40] and Ref.[20] for a detailed analysis). A modification of the C-C TB hopping at the edges is also included in the TB Hamiltonian following Ref.[31] to simulate the edge passivation, that yields a small energy gap at the charge neutrality point (CNP). As shown in Figure 1, the conductance for a single dopant (in various ribbon symmetries and impurity location) computed by our TB models nicely reproduces the *ab initio* transport calculations performed with the TABLIER code[40] for an extensive set of dopant positions and ribbons width. The conductance of long GNRs is then calculated within the Landauer-Büttiker formalism.[41] Order(N) decimation techniques are used to explore the various transport properties

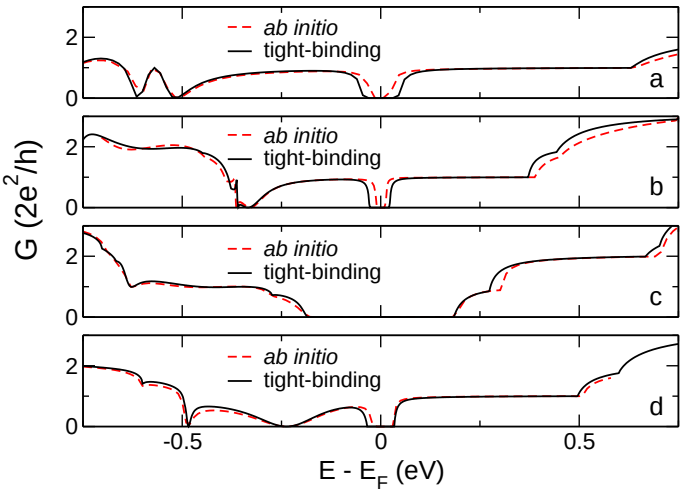


Figure 1: Conductance profile as a function of energy for the single-dopant case, both within the full *ab initio* approach (dashed red line) and the tight-binding model (solid black line) for the (a) 20-, (b) 35-, (c) 31- and (d) 26-aGNRs; the dopant has been placed at the (a) center, (b) midway between center and edge, (c) first neighbor to atom at edge, and (d) edge positions, respectively.

for randomly doped ribbons as long as 1 $\mu$m. By combining the accuracy of first-principles to describe the local electronic structure with the numerical efficiency of a nn-TB model, our transport methodology thus allows for a realistic exploration of the mesoscopic transport in randomly doped GNRs.

We first analyze the impact of different doping rates on ribbons of about 4 nm in width, namely the pseudo-metallic 35-aGNR and the semiconducting 34-aGNR. Ribbons with a length up to 1 $\mu$m are considered, and impurities are uniformly distributed over the whole ribbon length and width, with a restriction preventing the overlap of the scattering potentials of individual dopants. Figure 2 shows the conductance as a function of energy for the (a) 35- and (b) 34-aGNRs, for doping rates between $\approx$ 0.02% and 0.2%. In this formalism, electrodes are treated as semi-infinite, perfect GNRs, and disorder is included only in the region between the electrodes (channel). Since the scattering potential induces an overall shift of the CNP within the channel, the CNP of electrodes and channel are not aligned, leading to a displacement of the doping-induced gap with respect to that of the perfect ribbon. To properly analyze our results we have thus simply proceeded to a rigid

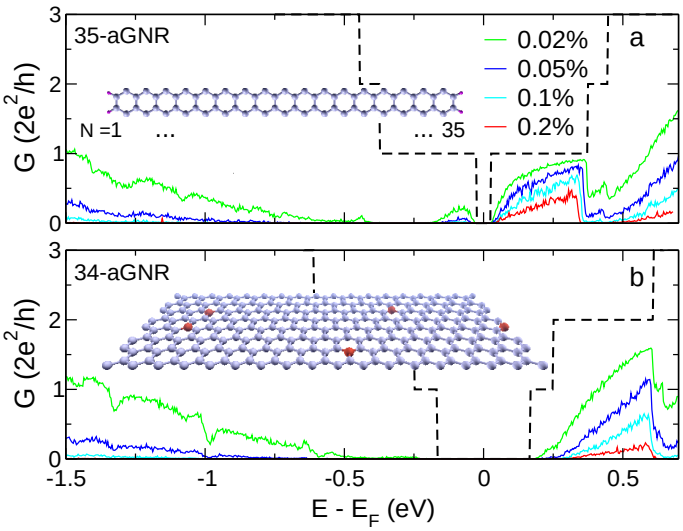


Figure 2: (a) Average conductance as a function of energy for the pseudo-metallic 35-aGNR for doping rates $\approx$ 0.02%, 0.05%, 0.1% and 0.2% (from top to bottom). The dashed black line corresponds to the ideal (undoped) case. The averages have been performed over $\approx$ 500 disorder realizations with a ribbon length of $\approx 1\ \mu$m. The inset shows the unit cell of the 35-aGNR with passivating H atoms. N indicates the number of dimer chains in a N-aGNR. (b) Same as in (a, main frame) for the semiconducting 34-aGNR. Inset: Schematic view of a randomly doped GNR.

shift of the conductance profile of the doped system to superimpose it to that of the ideal case. As a result of the acceptor-like character of the impurity states induced by the boron dopant, the conductance is affected in a clear asymmetric fashion for energy values below or above the CNP,[23] as evidenced by the opening of a large mobility gap that extends well beyond the first conductance *plateau* below the small initial electronic bandgap. The mobility gap width reaches almost 1 eV, of the order of the silicon energy gap.

Interestingly, despite the smaller size of the initial gap of the pseudo-metallic 35-aGNR with respect to that of the 34-aGNR, the magnitude of the doping-induced mobility gap in both ribbons is very similar for the same ribbon length and doping rate. This fact, as well as the higher conductance values for electron transport in the 35-aGNR (due to the robustness against scattering processes of the linear antibonding $\pi^*$ band in pseudo-metallic ribbons), make them even more suitable for their use in electronic devices.

Since the width of these GNRs is reaching the capability limits of standard lithographic techniques, we further explore the case of aGNRs with a width of $\approx$ 10 nm, namely the 80- and the

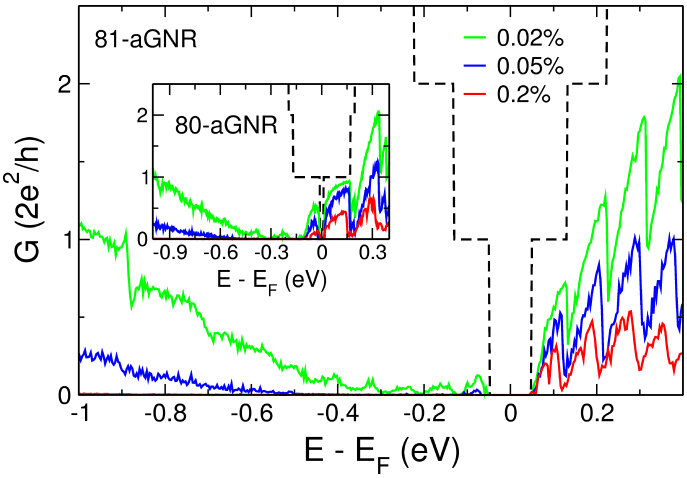


Figure 3: Main panel: Same as Figure 2 for the semiconducting 81-aGNR and three selected doping rates ($\approx$ 0.02%, 0.05% and 0.2%, from top to bottom). Inset: Same as in main frame for the pseudo-metallic 80-aGNR.

81-aGNR. For these systems, a doping rate below 0.2% is enough to achieve a mobility gap of $\approx$ 1 eV (see Figure 3, while keeping high conductance values in the conduction band for both types of wide GNRs. In this case, higher doping rates are required to achieve the full suppression of conductance in the valence band. This is due to the fact that backscattering in aGNRs is highly dependent on the dopant position, with a maximum impact when the dopant is close to (or right at) the ribbon edge.[23] As a consequence of a uniform random distribution of dopants, the probability to find an impurity close to the edges decreases with increasing ribbon width, and will be, for a 80-aGNR, almost one half than for a 35-aGNR, thus leading to a lower impact on the conductance for a similar doping rate.

The asymmetry in the electron *vs.* hole conduction[36,37] is also spectacularly evidenced by scrutinizing at the energy-dependent transport regimes. Figure 4 (main frame) shows the length dependence of the conductance for selected individual randomly doped 35-aGNRs, with a doping rate of $\approx$ 0.05%, at a energy = 0.25 eV below (a) and above (b) the CNP. For energy values lying in the conduction band (b), the conductance for various random configurations is seen to slowly decay with ribbon length with values staying close to the conductance quantum ($G_0 = 2e^2/h$), pinpointing a quasi-ballistic regime. Though all 1-dimensional systems show localization in the presence of disorder, for lower doping rates quantum interference effects are too weak to allow

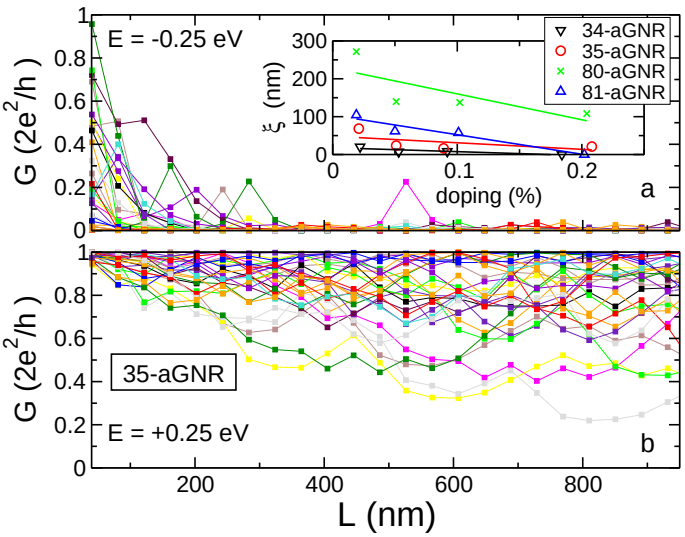


Figure 4: Main frame: Conductance as a function of length for a set of doping realizations of the 35-aGNR at 0.25 eV below (a) and above (b) the CNP for a doping rate of $\approx 0.05\%$. Curves with same color in (a) and (b) correspond to the same position of the dopants along the ribbon. Inset: Estimated localization lengths as a function of doping rate for the 34- and 35-GNRs (at E = -0.2 eV), and the 80- and 81-aGNRs (at E = -0.1 eV). Solid lines are fittings to the calculated values.

localization to manifest itself in the length scale considered in this study. In contrast, for energies lying in the valence band, a strong exponential decrease of the conductance is found (a), with large fluctuations associated to different defects positions. The exponential decay of the conductance with the length of the ribbon is related to the Anderson localization, that has already been observed experimentally at room temperature in defected metallic carbon nanotubes,[38] due to their long phase coherence lengths.

In the inset of Figure 4, the estimated localization lengths ($\xi$) for hole transport at different doping rates are reported. A statistical average over more than 500 disorder samples is performed to extract the $\xi$ from $\langle \ln G/G_0 \rangle = -\xi/L$, with $L$ the ribbon length. The localization length ranges within 10-300 nm, depending on the ribbon width and doping density, and is inversely proportional to the doping density. $\xi$ is also found to further increase with the ribbon width but in a non-linear fashion. This comes from the non-uniformity of the disorder potential with the dopant position.

In the case of carbon nanotubes, the localization length is predicted to increase linearly with the size of the system,[42] a trend confirmed experimentally.[43] A similar scaling law was derived in

pseudo-metallic GNRs.[44] This can be explained by invoking a generalization of Thouless relation for quasi-one dimensional systems, $\xi \sim N_{\perp} l_e$, where $N_{\perp}$ is the number of conducting modes available at a certain energy and $l_e$ is the elastic mean free path. In the first *plateau* around the CNP, ribbons of different widths present the same number of channels ($N_{\perp} = 1$), and $l_e$ is predicted to increase with the number of atoms in the unit cell,[44] thus leading to an increase of $\xi$. However, this is true only in the presence of a uniform disorder potential, which is not the case here. We note that similar power law scaling of $\xi$ has been observed for the case of edge disorder.[45,46]

In conclusion, we have performed a numerical transport study of boron doped armchair GNRs with widths up to $\approx$ 10 nm, and lengths reaching the micron scale and doping rates from 0.02% to 0.2%. Depending on the energy of charge carriers, the transport can vary from quasiballistic to a strongly localized regime, as a result of a strong electron/hole asymmetry induced by the chemical doping. This phenomenon leads to mobility gaps in the order of 1 eV, while the conductance in the conduction bands remains large, with values close to those of the ideal ribbon for low enough doping rates. This opens an unprecedented way to improve the performances of graphene-based devices since the obtained asymmetry should also manifest in a considerably higher ON/OFF current ratio. One notes that electron-hole conduction asymmetry in graphene devices by chemical functionalization has been recently reported by Farmer and coworkers,[37] whereas Raman studies of graphene-FETs allow for efficient monitoring of doping effects.[47]

## Acknowledgement

This work was supported by the GRAPHENE project of CARNOT Institute (LETI) and the ICT/FET European funding from GRAND and ANR-06-NANO-069-02 "Accent" projects. We thank the CEA/CCRT supercomputing facilities for providing computational resources.

# References

(1) Sze, S.M. *Physics of Semiconductor Devices* (Wiley, New York, 1981).

(2) Novoselov, K. S.; Geim, A. K.; Morozov, S. V.; Jiang, D.; Zhang, Y.; Dubonos, S. V.; Grigorieva, I. V.; Firsov, A. A. *Science* **2004**, *306*, 666.

(3) Berger, C.; Song, Z.; Li, X.; Wu, X.; Brown, N.; Naud, C.; Mayou, D.; Li, T.; Hass, J.; Marchenkov, A.N.; Conrad, E.H.; First, P.N.; de Heer, W.A. *Science* **2006**, *312*, 1191.

(4) Geim, A.K.; Novoselov, K.S. *Nature Materials* **2007**, *6*, 183.

(5) Ozyilmaz, B.; Jarillo-Herrero, P.; Efetov, D.; Abanin, D.A.; Levitov, L.S.; Kim, P. *Phys. Rev. Lett.* **2007**,*99*, 166804.

(6) Morozov, S.V.; Novoselov, K.S.; Katsnelson, M.I.; Schedin, F.; Elias, D.C.; Jaszczak, J.A.; Geim, A.K. *Phys. Rev. Lett.* **2008**, *100*, 016602.

(7) Castro Neto, A.H.; Guinea, F.; Peres, N.M.R.; Novoselov, K.S.; Geim, A.K. *Rev. Mod. Phys.* **2009**, *81*, 109.

(8) Fujita, M.; Wakabayashi, K.; Nakada, K.; Kusakabe, K. *J. Phys. Soc. Jpn.* **1996**, *65*, 1920.

(9) Nakada, K.; Fujita, M.; Dresselhaus, G.; Dresselhaus, M.S. *Phys. Rev. B* **1996**, *54*, 17954.

(10) Peres, N.M.R.; Castro Neto, A.H.; Guinea, F. *Phys. Rev. B* **2006**, *73*, 195411.

(11) Han, M.Y.; Özyilmaz, B.; Zhang, Y.; Kim, P. *Phys. Rev. Lett.* **2007**, *98*, 206805.

(12) Özyilmaz, B.; Jarillo-Herrero, P.; Efetov, D.; Kim, P. *Appl. Phys. Lett.* **2007**, *91*, 192107.

(13) Lemme, M.C.; Echtermeyer, T.J.; Baus, M.; Kurz, H. A. *IEEE Electron Device Letters* **2007**, *28*, 282.

(14) Chen, Z.; Lin, Y.-M.; Rooks, M.J.; Avouris, P. *Physica E* **2007**, *40*, 228.

(15) Kedzierski, J.; Hsu, P-L.; Healey, P.; Wyatt, P.W.; Keast, C.L.; Sprinkle, M.; Berger, C.; de Heer, W.A. *IEEE Transactions on Electron Devices* **2008**, *55*, 2078.

(16) Li, X.; Wang, X.; Zhang, L.; Lee, S.; Dai, H. *Science* **2008**, *319*, 1229.

(17) Wang, X.; Ouyang, Y.; Li, X.; Wang, H.; Guo, J.; Dai, H.*Phys. Rev. Lett.* **2008**, *100*, 206803.

(18) Schedin, F.; Geim, A.K.; Morozov, S.V.; Hill, E.W.; Blake, P.; Katsnelson, M.I.; Novoselov, K.S. *Nature Materials* **2007**, *6*, 652.

(19) Echtermeyer, T.J.; Lemme, M.C.; Baus, M.; Szafranek, B.N.; Geim, A.K.; Kurz, H. *et al. IEEE Elec. Dev. Lett.* **2008**, *29*, 952.

(20) Lherbier, A.; Blase, X.; Niquet, Y.-M.; Triozon, F.; Roche, S. *Phys. Rev. Lett.* **2008**, *101*, 036808.

(21) Robinson, J.P.; Schomerus, H.; Oroszlany, L.; Fal'ko, V.I. *Phys. Rev. Lett.* **2008**, *101*, 196803.

(22) Martins, T.B.; Miwa, R.H.; da Silva, A.J.R.; Fazzio, A. *Phys. Rev. Lett.* **2007**, *98*, 196803.

(23) Biel, B.; Blase, X.; Triozon, F.; Roche, S. *Phys. Rev. Lett.* **2009**, *102*, 096803.

(24) Yan, Q.; Huang, B.; Yu, J.; Zheng, F.; Zang, J.; Wu, J.; Gu, B.L.; Liu, F.; Duan, W. *Nano Lett.* **2007**, *7*, 1469.

(25) Gunlycke, D.; Li, J.; Mintmire, J.W.; White, C.T. *Appl. Phys. Lett.* **2007**, *91*, 112108.

(26) Cervantes-Sodi, F.; Csanyi, G.; Piscanec, S.; Ferrari, A.C. *Phys. Rev. B* **2008**, *77*, 165427.

(27) Kawai, T.; Miyamoto, Y.; Sugino, O.; Koga, Y. *Phys. Rev. B* **2000**, *62*, R16349.

(28) Koskinen, P.; Malola, S.; Häkkinen, H. *Phys. Rev. Lett.* **2008**, *101*, 115502.

(29) Wassmann, T.; Seitsonen, A.P.; Saitta, A.M.; Lazzeri, M.; Mauri, F. *Phys. Rev. Lett.* **2008**, *101*, 096402.

(30) Kobayashi, Y.; Fukui, K.I.; Enoki, T.; Kusakabe, K.; Kaburagi, Y. *Phys. Rev. B* **2005**, *71*, 193406.

(31) Son, Y.-W.; Cohen, M.L.; Louie, S.G. *Phys. Rev. Lett.* **2006**, *97*, 216803.

(32) Barone, V.; Hod, O.; Scuseria, G.E. *Nano Lett.* **2006**, *6*, 2748.

(33) White, C.T.; Li, J.; Gunlycke, D.; Mintmire, J.W. *Nano Lett.* **2007**, *7*, 825.

(34) Ewels, C.; Glerup, M. *J. Nanosci. Nanotech.* **2005**, *5*, 1345.

(35) Panchakarla, L.S.; Subrahmanyam, K.S.; Saha, S.K.; Govindaraj, A.; Krishnamurthy, H.R.; Waghmare, U.V.; Rao, C.N.R. *arXiv:0902.3077v1*.

(36) Park, C.-H.; Yang, L.; Son, Y.-W.; Cohen, M.L.; Louie, S.G. *Nature Physics* **2008**, *4*, 213.

(37) Farmer, D.B.; Golizadeh-Mojarad, R.; Perebeinos, V.; Lin, Y-M.; Tulevski, G.S.; Tsang, J.C.; Avouris, P. *Nano Lett.* **2009**, *9*, 388.

(38) Gómez-Navarro, C.; de Pablo, P.J.; Biel, B.; Garcia-Vidal, F.J.; Rubio, A.; Flores, F.; Gómez-Herrero, J. *Nature Materials* **2005**, *4*, 534.

(39) Avriller, R.; Latil, S.; Triozon, F.; Blase, X.; Roche, S. *Phys. Rev. B* **2006**, *74*, 121406(R).

(40) Adessi, Ch.; Blase, X.; Roche, S. *Phys. Rev. B.* **2006**, *73*, 125414.

(41) Datta, S. *Electronic Transport in Mesoscopic Systems* (Cambridge University Press, Cambridge, 1995).

(42) White, C.T.; Todorov, T.N. *Nature* **1998**, *393*, 240.

(43) Flores, F.; Biel, B.; Rubio, A.; Garcia-Vidal, F.J.; Gómez-Navarro, C.; de Pablo, P.J.; Gómez-Herrero, J. *J.Phys: Condens. Matter* **2008**, *20*, 304211.

(44) Areshkin, D.A.; Gunlycke, D.; White, C.T. *Nano Lett.* **2007**, *7*, 204.

(45) Evaldsson, M.; Zozoulenko, I.V.; Xu, H.; Heinzel, T. *Phys. Rev. B* **2008**, *78*, 161407(R).

(46) Mucciolo, E.R.; Castro Neto, A.H.; Lewenkopf, C.H. *Phys. Rev. B* **2009**, *79*, 075407.

(47) Das, A.; Pisana, S.; Chakraborty, B.; Piscanec, S.; Saha1, S.K.; Waghmare, U.V.; Novoselov, K.S.; Krishnamurthy, H.R.; Geim, A.K.; Ferrari, A.C.; Sood, A.K. *Nature Nanotech.* **2008**, *3*, 210.